High Gain, Low Dark Current $Al_{0.8}In_{0.2}As_{0.23}Sb_{0.77}$ Avalanche Photodiodes

Andrew H. Jones, Ann-Kathryn Rockwell, Stephen D. March, Yuan Yuan, Seth R. Bank, and Joe C. Campbell

***Abstract*— We report $Al_{0.8}In_{0.2}As_{0.23}Sb_{0.77}$ avalanche photodiodes with high gain (M >1300) and low dark current at room temperature. Impact ionization coefficients for this material system are also extracted, indicating electron-dominant impact ionization. Low avalanche breakdown temperature dependence is demonstrated.**

***Index Terms*— Avalanche photodiodes, photodetectors, telecommunication, fiber optic links and subsystems.**

I. Introduction

AVALANCHE photodiodes (APDs) have been widely deployed for use in telecommunication, military, and research applications including imaging and single-photon detection [1], [2]. The advantage of an APD compared to a PIN photodetector is its intrinsic gain, which manifests itself through the process of impact ionization. This stochastic process enables the detection of very weak signals but also affects the detector shot noise. The mean-squared shot noise current in an APD can be expressed as [3]

$$\langle i_{shot}^2 \rangle = 2q(I_{ph} + I_d)M^2F(M)\Delta f \quad (1)$$

where I_{ph} and I_d are the photocurrent and dark current respectively, M is the avalanche gain, $F(M)$ is the excess noise factor, and Δf is the bandwidth. In order to decrease the detector shot noise at high gain, both the excess noise factor and the dark current should be suppressed. The excess noise factor $F(M)$ is given by [3]

$$F(M) = kM + (1-k)(2 - {}^1/_M) \quad (2)$$

where k is the ratio of the electron and hole impact ionization coefficients α and β such that $k < 1$. Previously, $Al_xIn_{1-x}As_ySb_{1-y}$APDs have been reported with a low excess noise factor comparable to silicon [4]–[6]. The $Al_xIn_{1-x}As_ySb_{1-y}$ material system has a direct bandgap structure for x < 0.8, where it transitions to indirect bandgap. In this work, we report $Al_{0.8}In_{0.2}As_{0.23}Sb_{0.77}$(hereafter referred to as$Al_{0.8}$InAsSb)APDs with low dark current and high gain ($M > 1300$). The impact ionization coefficients are calculated as a function of electric field. We also report the temperature stability of these APDs. Due to the effects of phonon scattering, the electric field required to maintain a gain M increases with temperature. Ultimately, this corresponds to a proportional increase in the avalanche breakdown voltage with temperature. As a result, APDs are commonly characterized by their breakdown voltage temperature coefficient $\Delta V_{bd}/\Delta T$. In this work, we report a value of 5.4 mV/K for an $Al_{0.8}$InAsSb APD with a 1-μm multiplication layer, corresponding to an impact ionization temperature dependence 3 times lower than comparable InAlAs APDs [7].

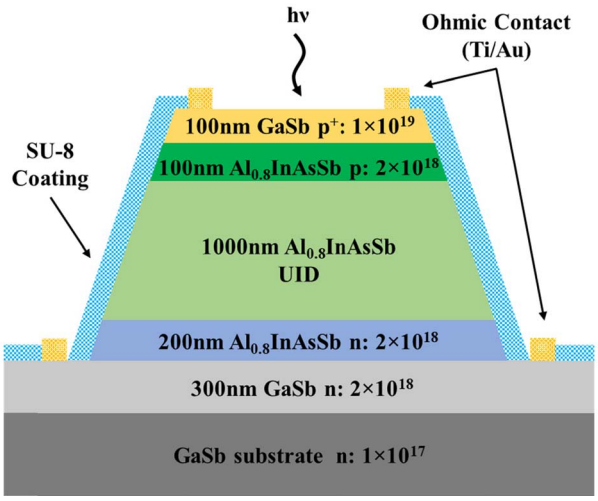

Fig. 1. Structural cross section of the $Al_{0.8}$InAsSb PIN APDs.

II. Experimental Details

A. Device Growth and Fabrication

The $Al_{0.8}$InAsSb epitaxial layers were grown on an n-type Te-doped GaSb (001) substrate by solid-source molecular beam epitaxy as a digital alloy of the binary semiconductors [8]. The multiplication layer thickness is 1 μm, as shown by the schematic cross section in Fig. 1.

Circular mesas were defined by standard photolithography and chemically etched with a citric/phosphoric acid solution.

Manuscript received August 12, 2019; revised September 9, 2019; accepted September 28, 2019. Date of publication November 6, 2019; date of current version December 19, 2019. This work was supported in part by the Army Research Office under Grant W911NF-17-1-0065 and in part by Defense Advanced Research Projects Agency (DARPA) under Grant GG11972.153060. *(Corresponding author: Joe C. Campbell.)*

A. H. Jones, Y. Yuan, and J. C. Campbell are with the Electrical and Computer Engineering Department, University of Virginia, Charlottesville, VA 22904 USA (e-mail: jcc7s@virginia.edu).

A.-K. Rockwell, S. D. March, and S. R. Bank are with the Electrical and Computer Engineering Department, The University of Texas at Austin, Austin, TX 78758 USA.

Color versions of one or more of the figures in this letter are available online at http://ieeexplore.ieee.org.

Digital Object Identifier 10.1109/LPT.2019.2950616

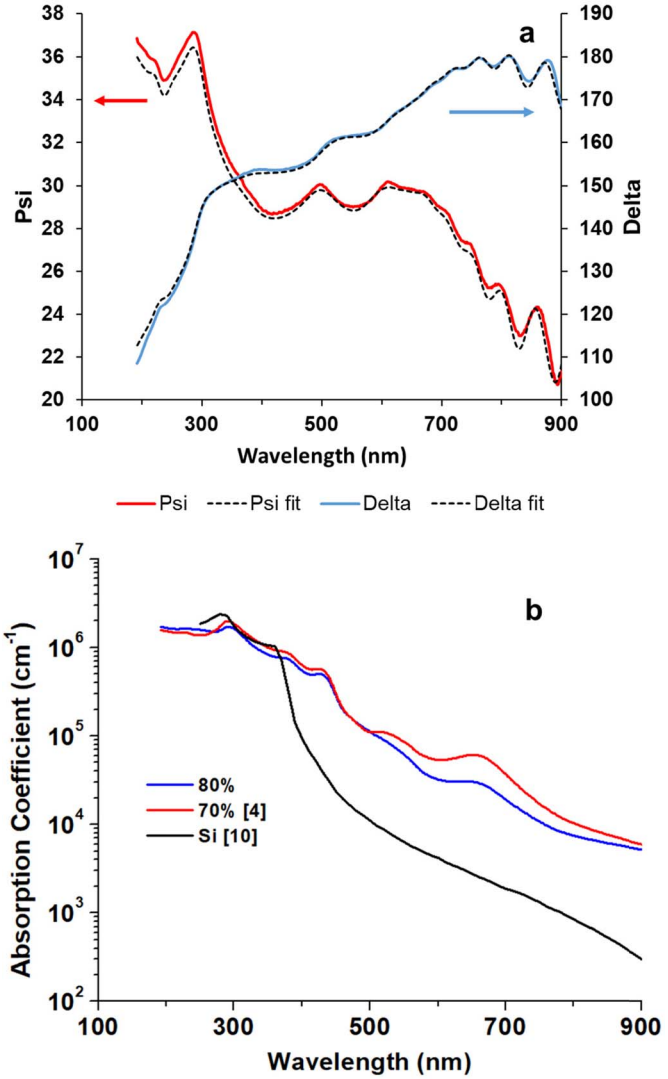

Fig. 2. Measured and fit ψ and Δ (a) and absorption coefficient (b) for $Al_{0.8}InAsSb$, $Al_{0.7}InAsSb$, and silicon.

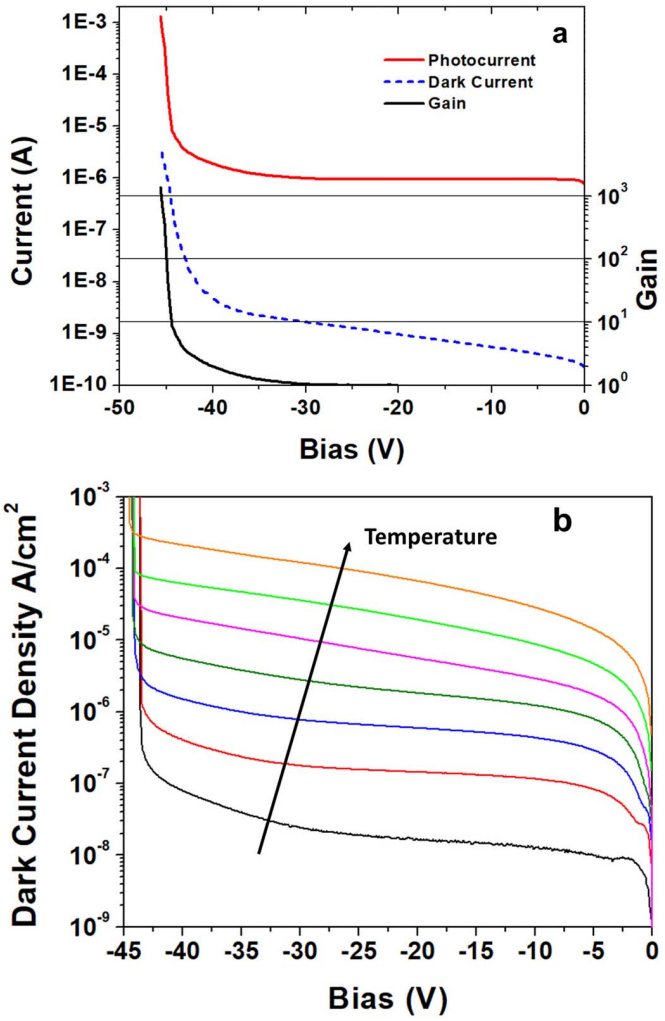

Fig. 3. (a) Dark current, photocurrent, and gain versus reverse bias of a 125-μm-diameter $Al_{0.8}InAsSb$ PIN APD at room temperature. (b) Current density for temperature from 220 K to 340 K in 20K increments.

A dilute bromine/methanol treatment was used to smooth the mesa sidewalls, and the devices were passivated with SU-8 to reduce surface leakage current. Ti/Au ohmic contacts were deposited using electron-beam evaporation.

B. Measurements

The $Al_{0.8}InAsSb$ was characterized by spectroscopic ellipsometry in order to determine the absorption coefficient, similarly to the technique described in [9]. This technique measures the amplitude ratio (ψ) and phase difference (Δ) between incident p and s-polarized light waves. These terms are related by the complex reflectance ratio (ρ) given by:

$$p = \tan(\psi)_e^{i\Delta}. \tag{3}$$

Ellipsometric measurements were made at a 60° incident angle.

Figure 2(a) shows the measured ψ and Δ values and a fitted model for each based on the epitaxial structure from Fig. 1. Figure 2(b) shows the calculated absorption coefficient of $Al_{0.8}InAsSb$ based on the shown models, compared to $Al_{0.7}InAsSb$ [9] and silicon [10]. While $Al_{0.7}InAsSb$ is recognized as a direct-bandgap material, $Al_{0.8}InAsSb$ may be slightly indirect, similar to silicon [8]. The absorption coefficient of $Al_{0.8}InAsSb$, however, is much greater than that of silicon and closer to that of $Al_{0.7}InAsSb$ in the visible and short-wave infrared spectrum.

In this letter, all devices were illuminated by an 850 nm vertical cavity laser unless otherwise indicated. Figure 3(a) shows the photocurrent, dark current and gain for a 125 μm-diameter APD. Gain was calculated by choosing the unity gain point at -20 V bias, which is before the onset of impact ionization and ensures full depletion of the intrinsic region. A gain in excess of $M = 1300$ was demonstrated before breakdown. The high gain is comparable to that of state-of-the-art HgCdTe APDs used for linear-mode, single-photon counting [11]. The current density versus bias is shown in Fig. 3(b) for temperature in the range 220 K to 340 K in 20 K increments. The high gain and low dark current suggest the potential for linear-mode single-photon counting. This is an ongoing field of study.

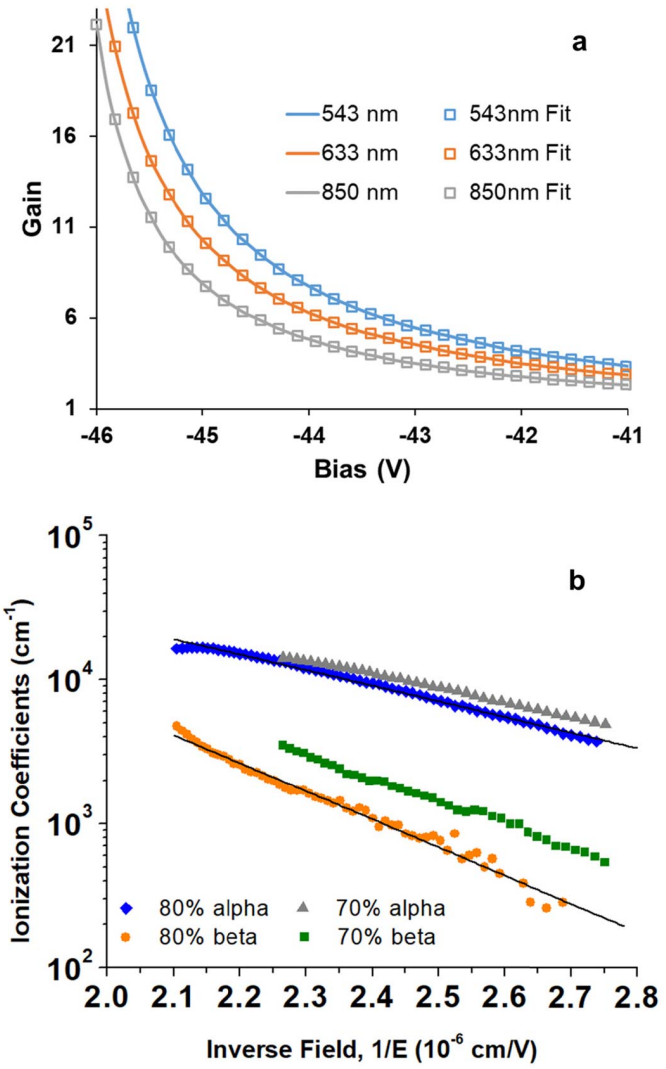

Fig. 4. (a) Measured gain curves under different illumination with fitted values from the impact ionization coefficients and (b) calculated impact ionization coefficients of $Al_{0.8}InAsSb$ and $Al_{0.7}InAsSb$ [9] including the best fit expressions given in equations (4) and (5).

To further characterize the previously demonstrated low excess noise characteristic of the $Al_{0.8}InAsSb$ material system, α and β where calculated using the pure-electron, pure-hole, and mixed injection method described in [12]. This methodology was also recently used to determine the impact ionization coefficients for $Al_{0.7}InAsSb$ [9]. The avalanche gain of $Al_{0.8}InAsSb$ was measured under 543, 850, and 633 nm illumination (for electron, hole, and mixed injection, respectively), and the impact ionization coefficients were extracted. While 850-nm illumination does not represent pure hole injection in this case, it is still sufficiently different from 543 and 633-nm illumination to allow for the reliable calculation of impact ionization coefficients [12]. Figure 4(a) shows the measured gain under the specified illumination and the simulated fit of these curves using the calculated coefficients, indicating good agreement. Figure 4(b) shows the calculated values for α and β as a function of inverse field in the multiplication region alongside the impact ionization coefficients for $Al_{0.7}InAsSb$ [9]. The electron impact ionization coefficient, α, is significantly higher than β, further confirming the low excess noise characteristics of this material system. Figure 4 shows that while the electron impact ionization coefficients for $Al_{0.8}InAsSb$ and $Al_{0.7}InAsSb$ are similar, the hole impact ionization coefficients for $Al_{0.8}InAsSb$ are even lower, indicating a lower excess noise figure for this wider-bandgap material. This agrees well with the theoretical findings that hole impact ionization in $Al_{0.7}InAsSb$ is suppressed by minibands in the valence band [13], and is further suppressed in the $Al_{0.8}InAsSb$ material. From this data, α and β for $Al_{0.8}InAsSb$ can be expressed analytically by the following best fit expressions, also shown in Figure 4(b):

$$a(E) = 3.66 \times 10^6 \times e^{-2.5\times10^6/E} \tag{4}$$

$$\beta(E) = 51.38 \times 10^6 \times e^{-4.49\times10^6/E} \tag{5}$$

We note that the ionization coefficients have been calculated in a limited field range from $\sim 2.1 \times 10^4$ to 2.8×10^4 cm/V.

Due to the low excess noise factor and dark current, these APDs offer the potential for high optical receiver sensitivity. The receiver sensitivity, P, in dBm was calculated for various bitrates by the following equation [14]:

$$P = 10\log\left[\left(\frac{h\upsilon}{q\eta}\right)\left(Q\cdot 10^3\right)\left(\frac{\langle i^2\rangle_c^{\frac{1}{2}}}{M} + qI_1QF(M)B\right)\right] \tag{6}$$

where υ is frequency, η is external quantum efficiency, Q is the signal-to-noise ratio, $\langle i^2\rangle_c^{1/2}$ is the sum of the amplifier and dark current noise, I_1 is the normalized noise-bandwidth integral, and B is the bandwidth. By assuming $Q = 6(10^{-9}$ bit error rate), $I_1 = 0.5$, external quantum efficiency of 0.45, and an amplifier input noise current of 0.8 μA at 10 Gb/s [15] and 2.42 μA at 25 Gb/s [16], the maximum receiver sensitivities at 10 Gb/s and 25 Gb/s were estimated to be – 31.3 dBm and – 26.9 dBm, respectively. This calculation is made at an operational gain of $M = 41$ and is based on an external quantum efficiency increase to 45.6% from the addition of an anti-reflection coating with ~1% reflectivity. At this gain, the excess noise factor is approximately $F(M) = 3.7$ [6].

The temperature stability of $Al_{0.8}InAsSb$ was investigated by measuring the gain from 220 to 340 K in increments of 20 K. The tested APDs were placed in a nitrogen-cooled cryogenic chamber in order to precisely control the ambient temperature. The breakdown voltage was determined from each measurement by extrapolating the inverse gain, I/M, to zero. A linear fit was applied to the resulting breakdown voltages, which indicates $\Delta V_{bd}/\Delta T = 5.4$ mV/K for a 1-μm multiplication region. This value is plotted in Fig. 5 alongside the indicated APD material systems as a function of multiplication layer thickness [7], [17]–[20]. The $\Delta V_{bd}/\Delta T$ for this material is 3 times lower than comparable InAlAs APDs and is projected to be approximately 8 times lower than comparable InP APDs [6]. The temperature stability may be due to the ultra-thin nature of the digital alloy superlattice. It has been shown that as the layer thicknesses of superlattices decrease, thermal conductivity is dominated by extrinsic processes and

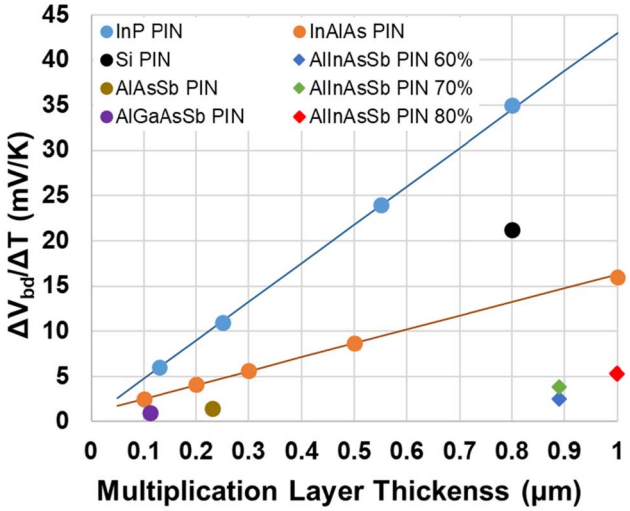

Fig. 5. $\Delta V_{bd}/\Delta T$ as a function of multiplication layer thickness for $Al_{0.8}InAsSb$ PIN APDs (this work) and others [7], [18]–[21].

that the nature of phonon scattering transitions from particle-like to wave-like, allowing for destructive phonon interference within the material [21], [22].

III. Conclusion

$Al_{0.8}InAsSb$ APDs demonstrate high gain, low dark current, low noise, and a low breakdown temperature coefficient. These characteristics in conjunction with the photoabsorption properties of $Al_{0.8}InAsSb$ make it an ideal material system for highly sensitive visible and near-infrared applications. These properties also make $Al_{0.8}InAsSb$ a promising candidate as the high-field region of a separate-absorption-charge-multiplication (SACM) APD for longer wavelength applications.

Acknowledgment

The authors would like to thank Dr. Patrick Hopkins at the Department of Electrical and Computer Engineering, University of Virginia for discussions regarding phonon scattering in digital alloy material.

References

[1] J. C. Campbell, "Recent advances in avalanche photodiodes," *J. Lightw. Technol.*, vol. 34, no. 2, pp. 278–285, Jan. 15, 2016.

[2] M. Ren *et al.*, "Laser ranging at 1550 nm with 1GHz sine-wave gated InGaAs/InP APD single-photon detector," *Opt. Express*, vol. 19, no. 14, pp. 13497–13502, Jul. 2011.

[3] R. J. McIntrye, "Multiplication noise in uniform avalanche photodiodes," *IEEE Trans. Electron Devices*, vol. ED-13, no. 1, pp. 164–168, Jan. 1966.

[4] M. Ren, J. S. Maddox, E. M. Woodson, Y. Chen, R. S. Bank, and C. J. Campbell, "Characteristics of $Al_xIn_{1-x}As_ySb_{1-y}$(x:0.3-0.7) avalanche photodiodes," *J. Lightw. Technol.*, vol. 35, no. 12, pp. 2380–2384, Jun. 15, 2017.

[5] M. Ren, S. J. Maddox, Y. Chen, S. R. Bank, M. Woodson, and J. C. Campbell, "AlInAsSb separate absorption, charge, and multiplication avalanche photodiodes," *Appl. Phys. Lett.*, vol. 108, no. 19, May 2016, Art. no. 191108.

[6] A.-K. Rockwell, Y. Yuan, A. H. Jones, S. D. March, S. R. Bank, and J. C. Campbell, "$Al_{0.8}In_{0.2}As_{0.23}Sb_{0.77}$ avalanche photodiodes," *IEEE Photon. Technol. Lett.*, vol. 30, no. 11, pp. 1048–1051, Jun. 1, 2018.

[7] L. J. J. Tan *et al.*, "Temperature dependence of avalanche breakdown in InP and InAlAs," *IEEE J. Quantum Electron.*, vol. 46, no. 8, pp. 1153–1157, Aug. 2010.

[8] S. J. Maddox, S. D. March, and S. R. Bank, "Broadly tunable AlInAsSb digital alloys grown on GaSb," *Cryst. Growth Des.*, vol. 16, no. 7, pp. 3582–3586, 2016.

[9] Y. Yuan, J. Zheng, A. K. Rockwell, S. D. March, S. R. Bank, and J. C. Campbell, "AlInAsSb impact ionization coefficients," *IEEE Photon. Technol. Lett.*, vol. 31, no. 4, pp. 315–318, Feb. 15, 2019.

[10] M. A. Green, "Self-consistent optical parameters of intrinsic silicon at 300 K including temperature coefficients," *Sol. Energy Mater. Sol. Cells*, vol. 92, no. 11, pp. 1305–1310, 2008.

[11] X. Sun *et al.*, "Single photon HgCdTe avalanche photodiode and integrated detector cooler assemblies for space lidar applications," *Proc. SPIE*, vol. 10659, pp. 1–14, May 2018.

[12] J. S. Ng, C. H. Tan, J. P. R. David, G. Hill, and G. J. Rees, "Field dependence of impact ionization coefficients in $In_{0.53}Ga_{0.47}As$," *IEEE Trans. Electron Devices*, vol. 50, no. 4, pp. 901–905, Apr. 2003.

[13] Y. Yuan *et al.*, "Comparison of different period digital alloy $Al_{0.7}InAsSb$ avalanche photodiodes," *J. Lightw. Technol.*, vol. 37, no. 14, pp. 3647–3654, Jul. 15, 2019.

[14] B. Kasper and J. Campbell, "Multigigabit-per-second avalanche photodiode lightwave receivers," *J. Lightw. Technol.*, vol. 5, no. 10, pp. 1351–1364, Oct. 1987.

[15] Inphi, Westlake Village, CA, USA, Product Datasheet: IN4701.

[16] Inphi, Westlake Village, CA, USA, Product Datasheet: IN2844TA.

[17] D. J. Massey, J. P. R. David, and G. J. Rees, "Temperature dependence of impact ionization in submicrometer silicon devices," *IEEE Trans. Electron Devices*, vol. 53, no. 9, pp. 2328–2334, Sep. 2006.

[18] A. H. Jones, Y. Yuan, M. Ren, S. Maddox, S. R. Bank, and J. C. Campbell, "$Al_xIn_{1-x}As_ySb_{1-y}$ photodiodes with low avalanche breakdown temperature dependence," *Opt. Express*, vol. 25, no. 20, pp. 24340–24345, 2017.

[19] S. Xie and C. H. Tan, "AlAsSb avalanche photodiodes with a sub-mV/K temperature coefficient of breakdown voltage," *IEEE J. Quantum Electron.*, vol. 47, no. 11, pp. 1391–1395, Nov. 2011.

[20] X. Zhou *et al.*, "Thin $Al_{1-x}Ga_xAs_{0.56}Sb_{0.44}$ diodes with extremely weak temperature dependence of avalanche breakdown," *Roy. Soc. Open Sci.*, vol. 4, no. 5, 2017, Art. no. 170071.

[21] A. Giri, J. L. Braun, D. M. Shima, S. Addamane, G. Balakrishnan, and P. E. Hopkins, "Experimental evidence of suppression of subterahertz phonons and thermal conductivity in GaAs/AlAs superlattices due to extrinsic scattering processes," *J. Phys. Chem.*, vol. 122, no. 51, pp. 29577–29585, 2018.

[22] J. Ravichandran *et al.*, "Crossover from incoherent to coherent phonon scattering in epitaxial oxide superlattices," *Nature Mater.*, vol. 13, no. 2, pp. 168–172, 2014.